

A RATE DEPENDENT EIGENEROSION PLASTICITY MODEL FOR CONCRETE

AUREL QINAMI* AND MICHAEL KALISKE†

*Institute for Structural Analysis, Technische Universität Dresden
01062 Dresden, Germany
e-mail: aurel.qinami@tu-dresden.de

†Institute for Structural Analysis, Technische Universität Dresden
01062 Dresden, Germany
e-mail: michael.kaliske@tu-dresden.de

Key words: Eigenerosion, Viscoplastic consistency model, Drucker-Prager with caps, Rate dependency

Abstract. In the publication at hand, a rate dependent plasticity model is introduced to describe the constitutive behavior of concrete. The smooth three surface Drucker-Prager yield function with caps is modified to account for the rate effects by use of the viscoplastic consistency model. Moreover, the fracture process is described via the eigenerosion approach in the framework of variational eigenfracture by coupling the failure with the evolution of plasticity. This is carried out by making the fracture surface energy dependent on the internal variable.

1 INTRODUCTION

The study of concrete material and its numerical characterisation has been a major field of research in the past decades. Upscaling the processes happening in the microstructure to capture a realistic response would at best, if all these processes are known, produce a very complicated and numerically inefficient model. Nonetheless, features like quasi-brittle fracturing and rate dependency, taken into account in this work, strongly determine the material behaviour at very high dynamic loading conditions.

The eigenfracture scheme, introduced in [1, 2], is a reliable method to model Griffith-like crack propagation which stems from the variational approach of fracture and has delivered very good results for static and dynamic loadings in elasticity, see [2, 3]. This work presents the extension of the approach to rate-dependent

plasticity material behaviour. Crucial is the determination of the crack-driving force based on the energetic description, where during the history of loading, a competition between the bulk energy and the surface fracture energy determines the crack propagation criterion and its direction. This is done by minimizing the total potential of the system, which gives rise to a binary element erosion, where an element can either be intact and carry loads or eroded and possesses no stiffness. The main advantages of the proposed approach are the straightforward implementation and its computation efficiency.

The bulk material is modelled via a rate dependent Drucker-Prager plasticity cap model. As depicted in [6], different mechanisms are present on the microscopic and structural level, which require loading rate dependency of the constitutive laws. This rate effect is considered by implementing a consistency model in the yielding surface, where its hardening depends

not only on the internal variable but also on its rate. Moreover, the constitutive relations are determined in the microplane framework in order to regard the induced anisotropy introduced by different evolutions of plasticity on each microplane.

The ability of the proposed formulation is tested via some numerical examples from literature and experiments. Despite the promising results at the current stage, further investigations of the mathematical eigenfracture description and validations of the model at more complex loading scenarios are necessary and part of our ongoing research.

2 THEORETICAL EVOLUTION

The core of this work is a twofold objective that starts with formulating a proper rate dependent material model for concrete in the framework of the microplane model and continues by describing the fracture phenomenon using the variational eigenfracture scheme initially introduced in [1].

2.1 Rate dependent Drucker-Prager yield surface with caps

An established technique to formulate the constitutive behavior of concrete is the microplane model. In this procedure, using e.g. the kinematic constraint, the macroscopic strain tensor is projected onto each microplane and decomposed into a volumetric and deviatoric part, namely, ϵ_V and ϵ_D , respectively. By utilizing a microplane energy functional, one can calculate the microplane stresses and tangent moduli on the basis of thermodynamic principles. Finally, all the microplane quantities can be homogenized by using a specific numerical integration to calculate the macroscopic values. In this work, we adopt the three surface smooth Drucker-Prager yield function, fully elaborated in [7], and formulate the rate dependent constitutive description of concrete. Thereby, we start with the representation of the macroscopic

stress tensor

$$\boldsymbol{\sigma} = \frac{3}{4\pi} \int_{\Omega} [K^{mic} \mathbf{V} (\epsilon_V - \epsilon_V^{vp})^2 + 2G^{mic} \mathbf{Dev}^T \cdot (\epsilon_D - \epsilon_D^{vp}) \cdot (\epsilon_D - \epsilon_D^{vp})] d\Omega, \quad (1)$$

with the volumetric projection tensor \mathbf{V} and the deviatoric one \mathbf{Dev} . The viscoplastic inelastic strains are represented by ϵ_V^{vp} and ϵ_D^{vp} . K^{mic} and G^{mic} are the microplane bulk and shear modulus. The integration over a total number of 42 microplanes takes place over the domain Ω , which, in the finite element setting, is the integration point.

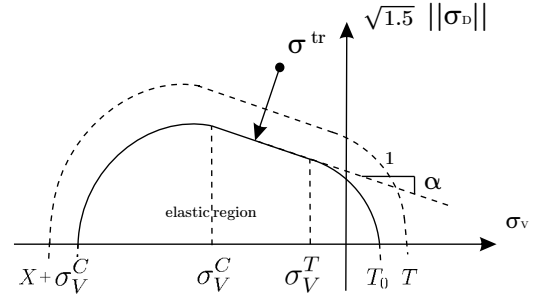


Figure 1: Drucker-Prager yield function with caps.

Fig. 1 represents the yield function in the microplane that reads

$$f^{mic} = \frac{3}{2} \boldsymbol{\sigma}_D^e \cdot \boldsymbol{\sigma}_D^e + f_1^2(\sigma_V^e, \kappa, \dot{\kappa}) f_c(\sigma_V^e, \kappa, \dot{\kappa}) f_t(\sigma_V^e, \kappa, \dot{\kappa}), \quad (2)$$

which depends on the microplane deviatoric elastic stresses $\boldsymbol{\sigma}_D^e$, volumetric elastic stresses σ_V^e , hardening internal variable κ and its rate $\dot{\kappa}$. The three functions in the second part of Eq. (2) are the standard Drucker-Prager surface f_1 , compression cap f_c and tension cap f_t that respectively read

$$\begin{aligned} f_1(\sigma_V^e, \kappa, \dot{\kappa}) &= \sigma_0 - \alpha \sigma_V^e + H\kappa + Y\dot{\kappa}, \\ f_c(\sigma_V^e, \kappa, \dot{\kappa}) &= 1 - H_c (\sigma_V^C - \sigma_V^e) \frac{(\sigma_V^e - \sigma_V^C)}{X^2}, \\ f_t(\sigma_V^e, \kappa, \dot{\kappa}) &= 1 - H_t (\sigma_V^e - \sigma_V^T) \frac{(\sigma_V^e - \sigma_V^T)}{(T - \sigma_V^T)^2}. \end{aligned} \quad (3)$$

In this formulation, hardening of the material depends on the evolution of variable κ and its rate $\dot{\kappa}$. This representation of the rate effect is known as the consistency viscoplastic formulation, see [8, 9]. In Eq. (3), Y is a hardening modulus which is calculated from the initial yield stress σ_0 and the viscosity parameter η as

$$Y = \eta \sigma_0. \quad (4)$$

Due to the fact that this is a brief introduction of our research, the explanation for the rest of material parameters in Eq. (3) can be found in [7]. The evolution of the volumetric and deviatoric inelastic strains is formulated using the plastic multiplier λ and the flow directions m_v and m_D . On the other hand, the hardening parameter κ has a simple linear dependence on the plastic multiplier. Thus, one can write

$$\begin{aligned} \dot{\epsilon}_V^{vp} &= \dot{\lambda} \frac{f^{mic}}{\partial \sigma_V^e} = \dot{\lambda} m_V, \\ \dot{\epsilon}_D^{vp} &= \dot{\lambda} \frac{f^{mic}}{\partial \sigma_D^e} = \dot{\lambda} m_D, \\ \dot{\kappa} &= \dot{\lambda}. \end{aligned} \quad (5)$$

If a stress state, represented by the trial values $\sigma_V^{e,tr}$ and $\sigma_D^{e,tr}$, lies outside the yield surface ($f^{mic} > 0$), a return mapping algorithm should project these values onto the yield surface values $\sigma_V^{e,n+1}$ and $\sigma_D^{e,n+1}$, where $n+1$ refers to the current time step. By exploiting a backward Euler scheme, the current stresses and hardening variables are calculated as

$$\begin{aligned} \sigma_V^{e,n+1} &= \sigma_V^{e,tr} - K^{mic} \epsilon_V^{vp,n+1}, \\ \sigma_D^{e,n+1} &= \sigma_D^{e,tr} - 2 G^{mic} \epsilon_D^{vp,n+1}, \\ \kappa^{n+1} &= \kappa^n + \Delta \lambda^{n+1}. \end{aligned} \quad (6)$$

Eqs. (6) combined with ($f^{mic} > 0$) form a nonlinear system of equations that can be solved by a local Newton-Raphson iterative scheme. The rate of the internal variable at the current time step is calculated as

$$\dot{\kappa} = \frac{\Delta \lambda^{n+1}}{\Delta t}. \quad (7)$$

The accumulation of plasticity for the integration point is given from the homogenized value of the internal variable as

$$\kappa^{hom} = \frac{\frac{3}{4\pi} \int_{\Omega} \kappa d\Omega}{\frac{3}{4\pi} \int_{\Omega} d\Omega}. \quad (8)$$

2.2 Eigenerosion formulation

Eigenerosion is a version of the eigenfracture scheme, presented in [1], that originates from the variational fracture. A regularized energy functional that combines the stored energy and the fracture surface energy is constructed in terms of the Γ -convergence setting. The basic idea of the scheme is that an eigendeformation field is used to describe the non continuous part of the domain (e.g. cracks) for the crack-tracking problem. As a result, the minimization with respect to the displacement and crack fields, automatically delivers the necessary equations for the mechanical and fracture solutions. For the sake of simplicity, in the following we will give the essence of the approach for the case of rate dependent plasticity model. The details of the technique and several applications can be found in [1–3]. The Griffith-like energetic criterion for the eigenerosion approach can be summarized in the discretized setting for an element K in

$$- \Delta F_K = - \Delta E_K - f(\kappa) G_c \cdot \Delta A_K, \quad (9)$$

with the energy release rate G_c , $-\Delta E_K$, the released energy for erosion of an element and neighbourhood support ΔA_K , which actually represents the nonlocal surface of a crack increment. The notion of nonlocality is used due to the fact that the calculation of the fracture surface energy does not depend only on the element itself, but also on its neighbourhood. The scaling function for the surface fracture energy reads

$$f(\kappa) = \frac{1}{1+p}, \quad (10)$$

where

$$p = \frac{\hat{\kappa}^{hom}}{\kappa_{crit}^{hom}}. \quad (11)$$

$\hat{\kappa}^{hom}$ is the maximum value of κ^{hom} among all integration points of element K . This coupling

of erosion with plasticity is motivated by the fact that concrete cannot carry indefinite plastic strains. Hence, the increase of these inelastic strains should encourage erosion. A fair approximation for ΔE_K can be calculated as

$$\Delta E_K = \int_{\bar{\Omega}} \Psi^{mac} d\bar{\Omega}, \quad (12)$$

with the homogenized macroscopic free energy

$$\begin{aligned} \Psi^{mac} &:= \frac{3}{4\pi} \int_{\Omega} \Psi^{mic} d\Omega \\ &= \frac{3}{4\pi} \int_{\Omega} [d' \frac{1}{2} K^{mic} (\epsilon_V - \epsilon_V^{vp})^2 \\ &\quad + d G^{mic} (\epsilon_D - \epsilon_D^{vp}) \cdot (\epsilon_D - \epsilon_D^{vp}) \\ &\quad + f(H, \kappa)] d\Omega, \end{aligned} \quad (13)$$

and the domain of integration for a specific element $\bar{\Omega}$. In Eq. (13), d and d' are given as

$$\begin{cases} d = 0 & \text{fracture} \\ d = 1 & \text{no fracture} \end{cases}, \quad (14)$$

$$\begin{cases} d' = 0 & tr(\epsilon_V) > 0 \\ d' = 1 & \text{otherwise} \end{cases}. \quad (15)$$

The contribution of the energy that comes from hardening is approximated as $f(H, \kappa) = 0.5 H \kappa^2$. In a fully thermodynamic consistent setting, erosion is applied to the macroscopic stress tensor

$$\begin{aligned} \sigma &= \frac{3}{4\pi} \int_{\Omega} [d' K^{mic} \mathbf{V} (\epsilon_V - \epsilon_V^{vp})^2 + \\ &\quad d 2 G^{mic} \mathbf{Dev}^T \cdot \\ &\quad (\epsilon_D - \epsilon_D^{vp}) \cdot (\epsilon_D - \epsilon_D^{vp})] d\Omega, \end{aligned} \quad (16)$$

and similarly for the effective tangent moduli. The procedure starts by checking for each element the criterion formulated in Eq. (9) for a given load step. If the accumulated energy overcomes the fracture barrier, the element is eroded by setting (partially) its stresses and stiffness to zero and solve the system for a new equilibrium. The above process is repeated in a frozen time step until no element from the mesh fulfils the

fracture criterion. After this, the load is updated for the next step. In this way, the eigenerosion approach works in a binary sense, meaning that an element in a given medium can either be intact and carry loads or be eroded by irreversibly losing its load bearing capacity.

3 NUMERICAL SIMULATION

3.1 Tensile test

The first numerical example introduced in this section is a tensile test of a concrete specimen with two parallel notches at the mid-height of the sample. This theoretical example is utilized to show the rate dependency of the proposed model and its contemplation in failure mechanism. Fig. 2 shows the boundary conditions and geometry of the analysed specimen, where the dimensions' unit is [mm]. Different displacement rates are applied at the top part of the specimen while the bottom part is clamped. Table 1 shows the used parameters of the proposed material model. The critical energy release rate is chosen as $G_c = 6.5 \cdot 10^{-2}$ kN/mm and the critical value of the homogenized hardening variable as $\kappa_{crit}^{hom} = 1.0 \cdot 10^{-6}$. The material parameters are chosen arbitrarily in a range that maintains general characteristics of concrete.

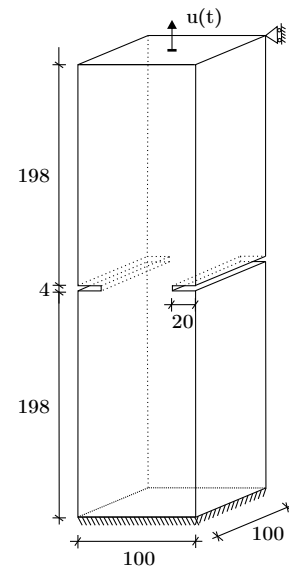
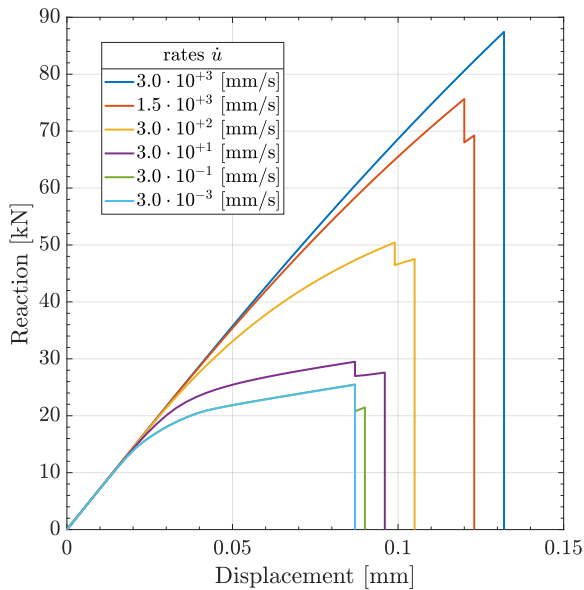
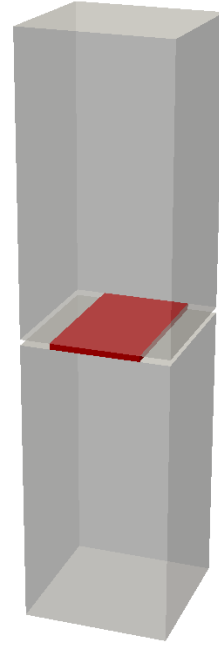


Figure 2: Specimen geometry of the tensile test.

Table 1: Material parameters for tensile test.

E [MPa]	30500
ν [-]	0.2
f_{uc} [MPa]	20
H [MPa]	$5.0 \cdot 10^4$
R_t [-]	1
σ_V^C [MPa]	-40
R [-]	2
η [s]	10.0

The focus of this example is the viscoplastic behavior of the material, hence, the wave propagation along the specimen under high rates will be neglected. This simplification does not impact the quality of results on the one hand, and emphasizes the viscoplastic nature of the proposed model on the other hand. The numerical simulations are performed under displacement controlled conditions. Six different rates are applied to the sample and the response in terms of reactions in loading direction and displacement at the top is inspected. Fig. 3 depicts graphically the achieved results. Due to the nature of this example, the reader should not make a quantitative relation to a specific type of concrete, but rather qualitatively observe the rate effects.

**Figure 3:** Load displacement curves for different rates.**Figure 4:** Mode I crack pattern.

For all the specimens, the Mode I failure mechanism is observed with a horizontal plane crack starting from the notches, see Fig. 4. As it is shown in Fig. 3, by increasing the loading rate, the behavior approaches closer to the elastic one. This hardening of the yield surface is attributed to the rate $\dot{\kappa}$, which prevents the evolution of plasticity. It is clear that for very low rates, the behavior is dominated only by elastoplasticity. Meanwhile, if the loading speed is raised, viscosity is activated and more elastic energy is stored inside the body. Moreover, one can notice in the graph an increase in strength that is only attributed to the material behavior. With the growth of viscous effects, dependency of fracture energy on plasticity decreases, which postpones the initiation of erosion. The role of viscosity in strength increase is one of the mechanisms in delaying fracture initiation in concrete. In literature, it is often reported that inertia plays a major role in the strength increase of concrete. For this reason, we examine in the next example the effects of structural inertia, introduced from the solution of the equation of motion, combined with the viscosity of the present model in a dynamic fracture problem.

3.2 Compact tension specimen (CT) under different rates

This example is chosen to show the effects of rate dependency on the crack patterns of a concrete compact tension specimen. The geometry and boundary conditions (BC) are shown in Fig. 5. At the bottom part of the notch, three different displacement rates \dot{u} are applied, specifically, 35 mm/s, 1300 mm/s and 4000 mm/s.

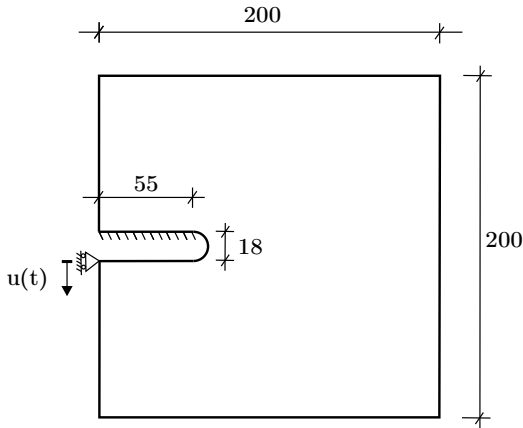


Figure 5: CT geometry and boundary conditions.

The chosen material parameters are given in Table 2. Moreover, the critical energy release rate takes the value $G_c = 5.5 \cdot 10^{-2}$ kN/mm and the critical value of the homogenized hardening variable is chosen as $\kappa_{crit}^{hom} = 1.0 \cdot 10^{-6}$. A specific number of elements at the load application is excluded from the erosion scheme in order

to avoid the failure of this region, which would deprive a correct load transfer into the body.

Table 2: Material parameters for CT specimen.

E [MPa]	30000
ν [-]	0.18
f_{uc} [MPa]	20
H [MPa]	$1.0 \cdot 10^4$
R_t [-]	1
σ_V^C [MPa]	-40
R [-]	2
η [s]	15.0

Newmark scheme is adopted for the solution of the time integration with the parameters $\beta = 0.5$ and $\gamma = 0.7$. These parameters introduce numerical damping in the solution of the equation of motion, but, for very high loading rates, this choice is necessary in order to maintain stability of the solution. For wave propagation and depending on the mesh size, the time step is calculated as $\Delta t = 7.0 \cdot 10^{-7}$ s.

The crack patterns for the experimental results, that are well documented in [5], are given in Fig. 6. The equivalent simulation results are depicted in Fig. 7. While the experimental setup includes two steel frames in each side of the notch to hold the sample and apply the load, in our simulations this takes place directly at the crack faces.

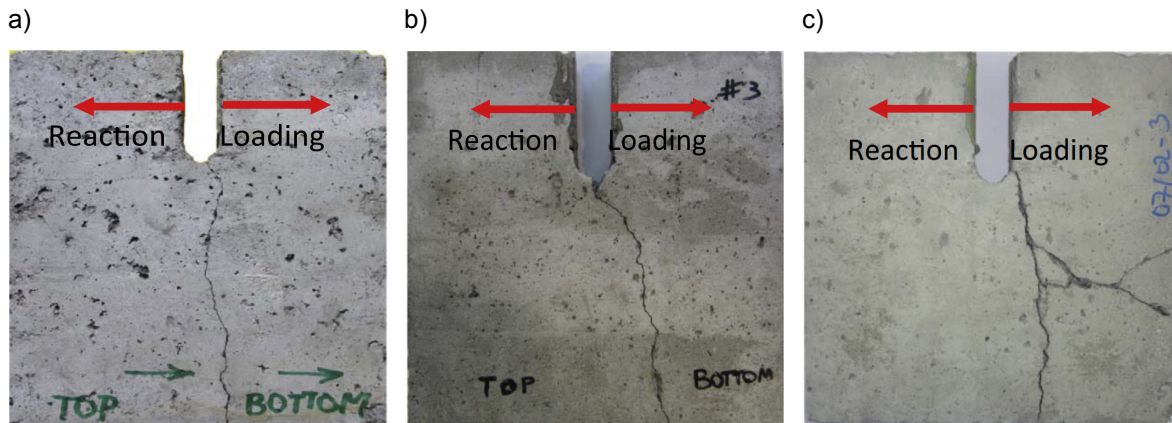


Figure 6: Experimental results extracted from [5] for loading rates a) 35 mm/s, b) 1300 mm/s and c) 3967 mm/s.

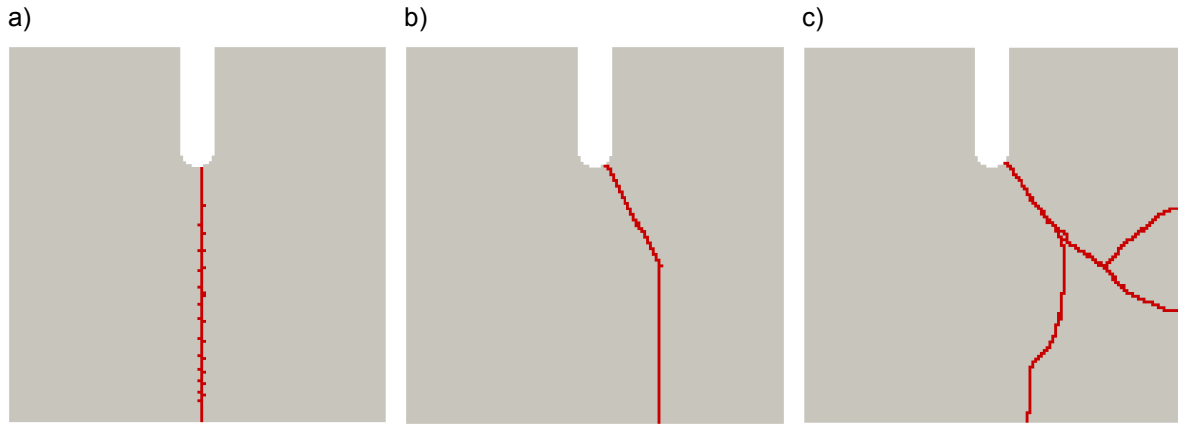


Figure 7: Simulation results for loading rates a) 35 mm/s, b) 1300 mm/s and c) 4000 mm/s.

It can be seen in Figs. 6 and 7, that crack patterns between experimental and simulation results match very well. Moreover, for almost static loading ($\dot{u} = 35$ mm/s), a purely Mode I cracking occurs and the energy is dissipated in the shortest possible path. When the loading rate increases, the energy accumulated at the crack tip also increases, requiring a larger crack surface for the energy dissipation, hence, the inclined crack in Fig. 7 b) is formed and a mixed mode cracking is achieved. Moreover, for the loading rate $\dot{u} = 4000$ mm/s, only one crack is not enough to dissipate the accumulated energy. As a result, branching occurs, see Fig. 7 c). In absence of the rate effects, no corresponding hardening evolution is present. Thus, the materials yield very early and plasticity develops in considerable scales. In this case, very thick crack patterns would be created due to the dependency of erosion on κ^{hom} . Thereby, the rate dependency not only provides a realistic constitutive material behavior, but also ensures a realistic crack pattern with the least dissipated fracture energy.

4 CONCLUSIONS

The current contribution introduces a rate dependent material formulation for concrete which is put in the framework of eigenerosion to provide crack-tracking. A smooth three surface Drucker-Prager yield function with caps is utilized to formulate the rate dependent problem. To this end, the consistency model is used

to describe viscoplastic behavior, where yield surface hardening occurs by an internal variable that describes plasticity and its rate. By always projecting on the yield surface, Kuhn-Tucker and consistency conditions are naturally fulfilled. Taking into account plasticity in the description of concrete behavior is motivated from evolution of small scale damage in the microstructure.

In order to account for the effects of plasticity evolution in the failure mechanism, the surface fracture energy is scaled by a function that depends on the internal variable. The existence of minimizers for this problem are ensured by the convexity of the energy functional. The regularization introduced by including the crack neighbourhood into calculation of the fracture energy avoids any mesh dependencies. The effects of mesh bias into crack propagation for the eigenerosion approach were introduced in [4], where adaptive refinement increases the possibilities of finding global minimizers for the fracture simulations. The introduced examples prove the capabilities of the proposed approach in terms of material description and crack patterns.

Acknowledgments

This work is supported by the German Research Foundation (DFG) within Research Training Group GRK 2250, Project B4.

REFERENCES

- [1] Schmidt, B., Fraternali, F., and Ortiz, M. 2009. Eigenfracture: an eigendeformation approach to variational fracture. *Multiscale Modeling and Simulation* **7**:1237–1266.
- [2] Pandolfi A., and Ortiz, M. 2012. An eigen-erosion approach to brittle fracture. *International Journal for Numerical Methods in Engineering* **92**:694–714.
- [3] Stochino, F., Qinami, A., and Kaliske, M. 2017. Eigenerosion for static and dynamic brittle fracture. *Engineering Fracture Mechanics* **182**:537–551.
- [4] Qinami, A., Bryant, E.C., Sun, W. and Kaliske, M., 2019. Circumventing mesh bias by r-and h-adaptive techniques for variational eigenfracture. *International Journal of Fracture*, <https://doi.org/10.1007/s10704-019-00349-x>.
- [5] Ožbolt, J., Bošnjak, J., and Sola, E. 2013. Dynamic fracture of concrete compact tension specimen: Experimental and numerical study. *International Journal of Solids and Structures* **50**:4270–4278.
- [6] Ožbolt, J., Sharma, A., Irhan, B., and Sola, E. 2014. Tensile behavior of concrete under high loading rates. *International Journal of Impact Engineering* **69**:55–68.
- [7] Zreid, I., and Kaliske, M. 2018. A gradient enhanced plasticity–damage microplane model for concrete. *Computational Mechanics* **62**:1239–1257.
- [8] Winnicki, A., Pearce, C.J., and Bićanić, N. 2001. Viscoplastic Hoffman consistency model for concrete. *Computer and Structures* **79**:7–19.
- [9] Wang, W.M. 1997. Stationary and propagative instabilities in metals - a computational point of view. PhD Thesis. Delft University of Technology.